ISME

An Exact Elastodynamic Solution for Functionally Graded Thick-Walled Cylinders Subjected to Dynamic Pressures

M. Shariyat †
Assosiate Professor

M.Nickkhah *
Gradute

In the present paper, an exact solution for transient response of an infinitely long functionally graded thick-walled cylinder subjected to dynamic pressures at the boundary surfaces is presented for arbitrary initial conditions. The cylinder is assumed to have a plane-strain condition and the dynamic pressures are assumed to be imposed uniformly and axisymmetrically on the boundary surfaces. Material properties of the cylinder are assumed to vary through the thickness according to a power law function. In contrast to many previous researches, the FGM cylinder is not divided into isotropic sub-cylinders. A solution approach associated with the expansion of the transient wave functions in terms of a series of the eigenfunctions is employed. The dynamic radial displacement expression is divided into quasi-static and dynamic parts and for each part, an analytical solution is presented. By this method, radial displacement and stress distributions in the functionally graded thick-walled cylinders are obtained for various values of the exponent of the power law function, various radius ratios, and various dynamic loads. Finally, advantages of the proposed method are discussed.

Key words: functionally graded materials, dynamic loads, eigen functions, thick-walled cylinder, Euler equation

1. Introduction

The main advantage of utilizing functionally graded materials (FGMs) is the capability to monitor variations of the volume fraction of the reinforcement phases within the microstructure of the mechanical components at the macroscopic or continuum scale. Therefore, functionally graded materials with arbitrary distributions (one dimensional, two dimensional, or even three dimensional distributions) of the constituent materials may be achieved based on the thermal, toughness, and strength requirements. Thick cylinders fabricated from functionally graded materials which are especially mixtures of ceramics and metals with continuous variations of the microstructure are commonly used. For FGM cylinders subjected to dynamic loads that may be

† Corresponding author, Associate Professor, Faculty of Mechanical Engineering, K.N. Toosi University of Technology, Pardis Street, Molla-Sadra Avenue, Vanak Square, Tehran, Iran.
E-mail: m_shariyat@yahoo.com and shariyat@kntu.ac.ir
* Graduate student, Faculty of Mechanical Engineering, K.N. Toosi University of Technology.

utilized in aerospace, nuclear, automobile, and other industries, analyzing the transient response is a vital stage.

Many of the well-known stress analyses performed so far for thick FGM cylinders are restricted to steady state thermoelastic analyses [1-3]. Some of these researches have been accomplished based on the multi-layer discretization approximation [4-6]. Limited researches have been presented for transient stress analysis of the FGM cylinders. Some researchers have investigated the transient thermal stresses using the classical thermal stress theory [4-13]. Eslami et al. have developed analytical solutions for thick isotropic cylinders and spheres [14]. They also have investigated the thermoelastic wave propagation in an FGM disc [15] that may be considered as a representative longitudinal portion of an infinitely long thick cylinder. Hosseini et al. [16] investigated the thermoelastic wave propagation phenomenon in thick-walled FGM cylinders with material properties that follow an exponential law, analytically.

Limited works have been developed in stress wave propagation analysis for the thick FGM cylinders. Heyliger and Jilania [17] adopted a variational method to study the frequency response of inhomogeneous cylinders and spheres. Han et al. [18] presented a hybrid numerical method for the analysis of transient waves in an FGM cylinder. The displacement responses were determined by employing the Fourier transformations. El-Raheb [19] studied effects of the circumferential and the radial inhomogeneities on the transient waves of a hollow cylinder. The cylinder is divided into isotropic subcylinders. The static-dynamic superposition method is employed to determine the transient response. Ponnusamy [20] discussed the wave propagation in a generalized thermoelastic isotropic solid cylinder with arbitrary cross-section. Shakeri et al. [21,22] studied vibration and transient behaviors of FGM thick hollow cylinders subjected to axisymmetric dynamic loads using a first order Galerkin finite element method. Hosseini [23] solved the mentioned problem analytically. As references [21] and [22], the functionally graded cylinder was divided into isotropic subcylinders. Although the idea of dividing the FGM cylinder into some isotropic sub-cylinders is commonly used, it may induce successive reflections and may affect the results. Bruck [24] and Samadhiya et al. [25] have proved that the elastic wave propagation in discretely layered FGMs is somewhat different. The transmitted wave and the reflected waves from each sharp interface between the discrete layers, may affect the stress distribution. Moreover, presence of the interfacial pressures and satisfying the continuity conditions in a multilayered circular cylinder or sphere cause additional difficulties in deriving the mathematical formulations of the analytical solutions. Recently, Shariyat [26] has proposed a nonlinear Hermitian transfinite element method for transient behavior analysis of hollow functionally gradad cylinders with temperature-dependent materials under thermo-mechanical loads.

Majority of the recent analytical studies have been carried out for FGM cylinders experiencing steady-state conditions. For instance, Tutuncu [27] developed an analytical solution for determination of the stress distributions in thick-walled FGM cylinders with exponentially varying properties. Transient plane-strain response of multilayered elastic cylinders subjected to axisymmetric impulse has been analyzed by Yue and Yin [28], using the expansion of transient wave functions in a series of eigenfunctions and Lamé's static solution. An analytical elastodynamic solution for spherically symmetric multilayered hollow spheres was presented by Ding et al. [29]. Recently, Tang and Cheng [30] studied elastodynamic response of an isotropic solid cylinder with mixed boundary surfaces analytically using the eigenfunction expansion method.

In the present paper, an analytical solution is presented to investigate the transient response of an infinitely long FGM thick-walled cylinder subjected to uniformly distributed dynamic pressures at the boundaries. To achieve this exact solution, a direct approach which leads to an Euler-type governing equation and expansion of the transient wave functions in a series in terms of the eigenfunctions is employed. In contrast to works performed so far, the

thick FGM cylinder is not divided into isotropic subcylinders. In the mentioned direct method the continuity conditions are satisfied automatically and in comparison to other techniques (e.g. the FEM and the transformation techniques), the computational time decreases remarkably. The present solution technique consists of decomposition of the radial displacement solution of the FGM cylinder into quasi-static and dynamic parts where for each part, an analytical solution is presented.

2. The governing equations

Consider an infinitely long thick-walled FGM cylinder with inner radius *a* and outer radius *b*. It is assumed that the cylinder is subjected to uniformly distributed dynamic pressures at the inner and outer boundary surfaces. Material properties of the cylinder are assumed to vary through the thickness according to the following power law function:

$$P = P_0(\frac{r}{b})^n \tag{1}$$

where P_0 is the reference property defined at the outer surface and *n* is a non-negative exponent of the power law function. In this paper, Young's modulus and the mass density are assumed to vary through the thickness according to Eq. (1), but Poisson's ratio assumed to be constant. To monitor the mechanical properties of the FGM cylinder through the thickness, the exponents of the power law function for Young's modulus and the mass density are considered to be distinct, so that:

$$E = E_0\left(\frac{r}{b}\right)^{n_1} \quad , \quad \rho = \rho_0\left(\frac{r}{b}\right)^{n_2} \tag{2}$$

For a plane-strain condition and an axisymmetric loading, in the absence of the body forces, the equation of motion is:

$$\frac{d\sigma_r}{dr} + \frac{\sigma_r - \sigma_\theta}{r} = \rho(r)\frac{\partial^2 u(r,t)}{\partial t^2} \tag{3}$$

where *u(r,t)* is the radial displacement component. For the mentioned axisymmetric problem, the strain-displacement relations are:

$$\varepsilon_r = \frac{du}{dr} \quad , \quad \varepsilon_\theta = \frac{u}{r} \tag{4}$$

The stress-strain equations have the following form:

$$\begin{aligned} \sigma_r &= c_1\varepsilon_r + c_2\varepsilon_\theta \\ \sigma_\theta &= c_2\varepsilon_r + c_1\varepsilon_\theta \end{aligned} \tag{5}$$

where, for the plane-strain conditions, c_1 and c_2 are:

$$\begin{aligned} c_1 &= \frac{E(r).(1-\nu)}{(1+\nu)(1-2\nu)} \\ c_2 &= \frac{\nu E(r)}{(1+\nu)(1-2\nu)} \end{aligned} \tag{6}$$

Substituting Eqs. (4) into Eqs. (5) and substituting the resulted equations in Eq. (3), lead to the Navier's equation of motion in terms of the radial displacement component:

$$\frac{\partial^2 u(r,t)}{\partial r^2} + (\frac{\partial c_1}{c_1 \partial r} + \frac{1}{r})\frac{\partial u(r,t)}{\partial r} + (\frac{\partial c_2}{r c_1 \partial r} - \frac{1}{r^2})u(r,t) = \frac{1}{c^2}\frac{\partial^2 u(r,t)}{\partial t^2} \tag{7}$$

c is the radial velocity of the stress wave (through the thickness) and is calculated according to the following equation:

$$c = \sqrt{\frac{c_1(r)}{\rho(r)}} = \sqrt{\frac{c_{10}}{\rho_0}} r^{\frac{n_1-n_2}{2}} \tag{8}$$

where c_{10} and ρ_0 are the reference elastic coefficient and mass density of the outer surface, respectively. By substitution of Eqs. (2), (6) and (8) in Eq. (7), one has:

$$\frac{\partial^2 u(r,t)}{\partial r^2} + (\frac{n_1+1}{r})\frac{\partial u(r,t)}{\partial r} + (\frac{\xi n_1 - 1}{r^2})u(r,t) = \frac{\rho_0}{c_{10}} r^{n_2-n_1} \frac{\partial^2 u(r,t)}{\partial t^2} \tag{9}$$

where $\xi = \frac{c_{20}}{c_{10}} = \frac{\nu}{1-\nu} = \text{const.}$ and $a \le r \le b$.

Boundary and initial conditions of the FGM thick-walled cylinder which is subjected to uniformly distributed dynamic pressures at its inner and outer surfaces are expressed as follows:

$$\begin{aligned} \sigma_r(a,t) &= -p_1(t) \\ \sigma_r(b,t) &= -p_2(t) \\ u(r,0) &= u_0(r) \\ v(r,0) &= v_0(r) \end{aligned} \tag{10}$$

where $\sigma_r(r,t)$, $u_0(r)$ and $v_0(r)$ are the radial stress, the initial radial displacement, and the initial radial velocity, respectively.

3. The proposed analytical solution

To find an exact solution for Eq. (9) based on the boundary and the initial conditions defined in Eq. (10), solution of the dynamic radial displacement $u(r,t)$ is divided into quasi-static $u_{st}(r,t)$ and dynamic $u_{dy}(r,t)$ parts. The quasi-static part $u_{st}(r,t)$ satisfies the static (steady state) equilibrium equation and the imposed boundary tractions. The dynamic part $u_{dy}(r,t)$ satisfies the motion equation and the stress-free boundary conditions (to some extent, it is the transient response). Finally, the dynamic radial displacement is expressed in a series of the eigenfunctions as follows [31,32]:

$$u(r,t) = u_{st}(r,t) + u_{dy}(r,t) = u_{st}(r,t) + \sum_{i=1}^{\infty} U_i(r)\Psi_i(t) \tag{11}$$

where $U_i(r)$ is the ith wave mode of the FGM thick-walled cylinder and $\Psi_i(t)$ is the unknown time-dependent coefficient associated with the $U_i(r)$ function. In order to obtain an exact solution of the whole dynamic radial displacement expression $u(r,t)$, it is necessary to find both the quasi-static and the dynamic parts.

3.1. The quasi-static part

The quasi-static radial displacement may be obtained by solving the following steady-state equilibrium equation and the relevant boundary conditions:

$$\frac{\partial^2 u_{st}(r,t)}{\partial r^2} + (\frac{n_1+1}{r})\frac{\partial u_{st}(r,t)}{\partial r} + (\frac{\xi n_1 - 1}{r^2})u_{st}(r,t) = 0 \tag{12}$$

$$\sigma_r(a,t) = -p_1(t) \quad , \qquad \sigma_r(b,t) = -p_2(t) \tag{13}$$

The above equation is Euler's equation with constant coefficients and may be solved easily as follows:

$$u_{st}(r,t) = Ar^{\eta} \tag{14}$$

By substitution Eq. (14) into Eq. (12), a characteristic equation is obtained whose roots are ex-

ponents of Eq. (14):

$$\eta^2 + n_1\eta + (\xi n_1 - 1) = 0$$
$$\eta_1, \eta_2 = \frac{-n_1 \pm \sqrt{n_1{}^2 - 4\xi n_1 + 4}}{2} \tag{15}$$

Hence, the quasi-static part of the whole radial displacement expression is obtained as follows:

$$u_{st}(r,t) = A(t)r^{\eta_1} + B(t)r^{\eta_2} \tag{16}$$

A(t) and *B(t)* are the unknown time-dependent coefficients that may be obtained based on the boundary conditions (13).

3.2. The dynamic part

In order to obtain the dynamic part of the whole radial displacement solution, it is necessary to find the governing equations of the wave modes and the unknown time-dependent coefficients, and satisfying the orthogonality conditions of the wave modes. The wave modes $U_i(r)$ are governed by the following eigenvalue equation:

$$\frac{d^2U(r)}{dr^2} + (\frac{n_1+1}{r})\frac{dU(r)}{dr} + (\frac{\xi n_1 - 1}{r^2})U(r) = -\frac{\rho_0\omega^2}{c_{10}} r^{n_2-n_1}U(r) \tag{17}$$

By definition of the following parameter:

$$k^2 = \frac{\rho_0\omega^2}{c_{10}} \tag{18}$$

Equation (17) becomes:

$$\frac{d^2U(r)}{dr^2} + (\frac{n_1+1}{r})\frac{dU(r)}{dr} + (k^2 r^{n_2-n_1} + \frac{\xi n_1 - 1}{r^2})U(r) = 0 \tag{19}$$

where boundary conditions relevant to Eq. (19) are chosen corresponding to stress-free boundary surfaces:

$$\sigma_r(a,\omega) = 0 \quad , \quad \sigma_r(b,\omega) = 0 \tag{20}$$

It may readily be shown that the eigenvalue ω^2 is a real non-negative number [33]. The general solution of (16) according to Bessel's equations is [34]:

$$U(r) = D\varepsilon_\alpha(\lambda r^q) \tag{21}$$

where:

$$\varepsilon_\alpha(\lambda r^q) = r^{-\frac{n_1}{2}}(\beta_1 J_\alpha(\lambda r^q) + \beta_2 Y_\alpha(\lambda r^q))$$
$$q = \frac{2 + n_2 - n_1}{2}$$
$$\lambda = \frac{2k}{2 + n_2 - n_1} \tag{22}$$
$$\alpha = \frac{\sqrt{n_1{}^2 - 4\xi n_1 + 4}}{2 + n_2 - n_1}$$

$J_\alpha(\lambda r^q)$ and $Y_\alpha(\lambda r^q)$ are Bessel's functions of the first and the second kinds of the αth order, respectively. β_1 and β_2 are unknown coefficients that are obtained by incorporation of the stress-free boundary conditions (20). Indeed, based on Eqs. (4) to (6) and (21), one may write:

$$\sigma_r(r,\omega) = c_1(r)\frac{\partial U(r,\omega)}{\partial r} + c_2\frac{U(r,\omega)}{r} = \left[c_1(r)\left(\frac{-n_1}{2}r^{-(1+\frac{n_1}{2})} + r^{-\frac{n_1}{2}}\frac{\partial}{\partial r}\right) + c_2(r)r^{-(1+\frac{n_1}{2})}\right] \tag{23}$$
$$.\left[\beta_1 J_\alpha(\lambda r^q) + \beta_2 Y_\alpha(\lambda r^q)\right]$$

It may be easily verified that [34]:

$$\frac{\partial}{\partial r}\left[J_\alpha\left(\lambda r^q\right)\right]=\left[J_{\alpha-1}\left(\lambda r^q\right)-\frac{\alpha}{\lambda r^q}J_\alpha\left(\lambda r^q\right)\right]\lambda q r^{q-1}$$
$$\frac{\partial}{\partial r}\left[Y_\alpha\left(\lambda r^q\right)\right]=\left[Y_{\alpha-1}\left(\lambda r^q\right)-\frac{\alpha}{\lambda r^q}Y_\alpha\left(\lambda r^q\right)\right]\lambda q r^{q-1} \tag{24}$$

Substituting Eq. (24) into Eq. (23), leads to the following result:

$$\sigma_r(r,\omega)=\left[c_1(r)\left(\frac{-n_1}{2}-\alpha q\right)+c_2(r)\right]r^{-(1+\frac{n_1}{2})}\left[\beta_1 J_\alpha(\lambda r^q)+\beta_2 Y_\alpha(\lambda r^q)\right]$$
$$+c_1\lambda q(r)r^{q-\frac{n_1}{2}-1}\left[\beta_1 J_{\alpha-1}(\lambda r^q)+\beta_2 Y_{\alpha-1}(\lambda r^q)\right] \tag{25}$$

or:

$$\sigma_r(r,\omega)=\beta_1\Lambda_1(r)+\beta_2\Lambda_2(r) \tag{26}$$

By substitution of Eq. (26) into the stress-free boundary conditions (20), a set of linear algebraic equations may be obtained:

$$\begin{bmatrix}\Lambda_1(a,\omega) & \Lambda_2(a,\omega)\\ \Lambda_1(b,\omega) & \Lambda_2(b,\omega)\end{bmatrix}\begin{Bmatrix}\beta_1\\ \beta_2\end{Bmatrix}=\begin{Bmatrix}0\\ 0\end{Bmatrix} \tag{27}$$

Eq. (27) may be written in the following compact form:

$$[\Lambda]\{\beta\}=\{0\} \tag{28}$$

where $\{\beta\}$ is an eigenvector. Existence of the nontrivial solutions requires that the determinant of the $[\Lambda]$ matrix becomes zero:

$$|\Lambda|=0 \tag{29}$$

Eq. (29) gives a transcendental equation that is the characteristic equation (or frequency equation) of the axisymmetric plane-strain radial vibration of the infinitely long FGM thick-walled cylinder. Rao [32] has shown that an elastic body has infinite positive characteristic values, so that the characteristic equation of the FGM cylinder has infinite number of positive roots. The positive roots of the mentioned equation provides the values of ω_i (i=1,2,3,…) which represent the circular frequencies or the eigenvalues of the cylinder. The circular frequencies may be determined accurately from the characteristic or frequency Eq. (29) by numerical methods such as Newton-Raphson method.

The *i*th vibrational mode of the FGM thick-walled cylinder $U_i(r)$ associated with the *i*th circular frequency ω_i may be expressed by the following equation:

$$U_i(r)=D_i\varepsilon_\alpha(\lambda_i r^q)$$
$$\varepsilon_\alpha(\lambda_i r^q)=r^{-\frac{n_1}{2}}\left[\beta_{1i}J_\alpha(\lambda_i r^q)+\beta_{2i}Y_\alpha(\lambda_i r^q)\right] \tag{30}$$

where β_{1i} and β_{2i} are unknown coefficients associated with circular frequency ω_i and may be determined by using Eq. (27).

The wave modes $U_i(r)$ form an orthogonal set. This set is derived directly from Eqs. (15) and (16) based on the following orthogonality condition that may be proved by using Eq. (19) and the stress-free boundary conditions:

$$\int_a^b \rho(r)U_i(r)U_j(r)2\pi r\,dr=\delta_{ij} \tag{31}$$

where δ_{ij} is the Kronecker delta function.

The coefficient D_i in Eq. (30) is obtained based on the orthogonality condition (31) as follows:

$$D_i^{-2} = \int_a^b \rho(r)\,\varepsilon_\alpha^{\,2}(\lambda_i r^q)\,2\pi r\,dr \tag{32}$$

Substituting Eq. (11) into Eq. (9) and employing the $u_{st}(r,t)$and $u_{dy}(r,t)$ expressions, lead to the following equation [31]:

$$\sum_{i=1}^{\infty}\left(\frac{d^2\Psi_i(t)}{dt^2}+\omega_i^{\,2}\Psi_i(t)\right)U_i(r)=-\frac{d^2u_{st}(r,t)}{dt^2} \tag{33}$$

The ordinary differential equations governing $\Psi_i(t)$ are obtained by using the orthogonality condition (31) as:

$$\begin{aligned}\frac{d^2\Psi_i(t)}{dt^2}+\omega_i^{\,2}\Psi_i(t)&=\frac{d^2\Phi_i(t)}{dt^2}\\ \Phi_i(t)&=-\int_a^b \rho(r)\,u_{st}(r,t)\,U_i(r)\,2\pi r\,dr\end{aligned} \tag{34}$$

It is now necessary to determine the initial conditions of $\Psi_i(t)$ in terms of the given initial conditions (10). It follows from Eq. (11) that:

$$\begin{aligned}u_0(r)&=u_{st}(r,0)+\sum_{i=1}^{\infty}U_i(r)\Psi_i(0)\\ v_0(r)&=\frac{du_{st}(r,0)}{dt}+\sum_{i=1}^{\infty}U_i(r)\frac{d\Psi_i(0)}{dt}\end{aligned} \tag{35}$$

Substituting the orthogonality condition (31) into Eq. (33) leads to:

$$\begin{aligned}\Psi_i(0)&=\int_a^b \rho(r)\,u_0(r)\,U_i(r)\,2\pi r\,dr+\Phi_i(0)\\ \frac{d\Psi_i(0)}{dt}&=\int_a^b \rho(r)\,v_0(r)\,U_i(r)\,2\pi r\,dr+\frac{d\Phi_i(0)}{dt}\end{aligned} \tag{36}$$

Hence solution of Eq. (34) based on the initial conditions (35) using the Laplace transform becomes:

$$\Psi_i(t)=\Psi_i(0)\cos\omega_i t+\frac{1}{\omega_i}\frac{d\Psi_i(0)}{dt}\sin\omega_i t+\frac{1}{\omega_i}\int_0^t\frac{d^2\Phi_i(\tau)}{d\tau^2}\sin\omega_i(t-\tau)\,d\tau \tag{37}$$

4. The solution procedure

Determination of the radial displacement and stress components using the presented elasto-dynamic solution may be accomplished according to the following steps:

1- The quasi-static radial displacement can be determined by using Eq. (16).

2- The circular resonant frequencies are calculated numerically by utilizing Eq. (29).

3- The corresponding coefficients and wave modes are determined based on Eqs. (27), (30) and (32).

4- The time-dependent functions $\Psi_i(t)$ are determined using Eq. (37).

5- The dynamic radial displacements are determined according to Eq. (11).

6- The stress components are obtained using Eqs. (4) and (5).

It is an evident that the numerical calculations have to be accomplished for a finite number of the wave modes (m). Therefore, Eq. (11) may be rewritten in the following form, for the mentioned purpose:

$$u(r,t)=u_{st}(r,t)+u_{dy}(r,t)=u_{st}(r,t)+\sum_{i=1}^{m}U_i(r)\Psi_i(t) \tag{38}$$

$m=50$ is adopted to extract results of the present paper.

5. Numerical Results

Example 1: As a first stage, an example of reference [26] is reexamined, for validation purposes. An infinitely long thick hollow FGM cylinder with inner radius *a=1[m]* and outer radius *b=1.2[m]* is considered. The reference modulus of elasticity and the reference mass density of the outermost layer are E_0=380 GPa and ρ_0=3800 kg/m^3 (mechanical properties of the alumina materials), respectively. The inner surface of the FGM cylinder is subjected to a uniformly distributed short-time pressure that increases linearly with time to a specified pressure [26]:

$$p_1(t) = p^* t \quad , 0 \le t \le t_0 \tag{39}$$

where p^* and t_0 are adopted as 4 (GPa/s) and 0.005 (s), respectively. Fig.1 shows the distribution of the radial stress through the thickness of the FGM cylinder at t=0.004 (s), for n_1=n_2=0.5 and b/a=1.2 along with results of the numerical method presented by Shariyat [26]. It is observed that good agreement between the results of the two methods is achieved.

Example 2: The FGM cylinder of example 1 is considered to be subjected to an exponential dynamic pressure imposed uniformly on the inner boundary surface. Therefore, the time histories of the pressures imposed on the inner and outer boundary surfaces may be expressed as:

$$\begin{aligned} p_1(t) &= p_0(1 - e^{-c_0 t}) \\ p_2(t) &= 0 \end{aligned} \tag{40}$$

where p_0 and c_0 are constants and are supposed to be 10 (MPa/s) and 1000 (s^{-1}), respectively.

Tables 1, 2, and 3 show the first six eigenvalues or natural frequencies of the infinitely long thick hollow FGM cylinders for various outer to inner radius ratios (*b/a)* and n_1=n_2=n. It may be easily seen that for the various values of the power law exponents, the eigenvalues decreases as the *b/a* ratio increases. Based on Eqs. (2), when the thickness of the hollow cylinder increases, values of the material properties of the innermost layer and subsequently the mean stiffness and the mass density through the thickness decrease and in overall, the resonant frequencies decrease. Furthermore, for a constant thickness, mean values of the stiffness and the mass density through the thickness decrease by an increase in the power law exponents, and therefore the fundamental natural frequency of the cylinder decreases.

Example 3: In the present example, sensitivity analyses are performed. An infinitely long thick hollow FGM cylinder with inner radius *a=1m* is considered and the results are extracted for various *b/a* ratios. The elastodynamic solutions of the FGM cylinders are determined for two distinct cases. In the first case, the exponents n_1 and n_2 are assumed to be identical. In the second case, it is assumed that the outer surface of cylinder is made of pure alumina (E_{Al2O3}=380 GPa and ρ_{Al2O3}=3800 kg/m^3) whereas the inner surface of cylinder is made of pure aluminium (E_{Al}=70 GPa and ρ_{Al}=2707 kg/m^3) and the properties are graded through the thickness from the inner surface to the outer one according to Eqs. (2). Therefore, in the latter case the exponents of the power law function for Young's modulus and the mass density vary with the radius ratio (e.g. for a thickness with ratios of b/a=1.2, it is noticed that n_1=9.2875 and n_2=1.86 and for a b/a=2 ratio, it is obtained that n_1=2.4406 and n_2=0.4893). Fig. 2 shows the distribution of the radial displacement through the thickness for various values of the power law exponents at time t=0.001 s, for b/a=1.2. The value of the power law exponent influences the amplitude of the radial displacement, directly. It is observed that the hollow cylinder made of alumina-aluminium FGM (n_1=9.2875 and n_2=1.86) has the greatest amplitude of the radial displacement. Fig. 3 illustrates time history of the radial displacement of the middle point of thick hollow FGM cylinder for various values of the power law exponents, b/a=1.2. The distribution of the radial displacement through the thickness of the FGM cylinder for various values of the power law exponents at time t=0.001 s, is shown in Fig. 4 for (b/a=2). It was mentioned that the material properties of the inner surface of FGM hollow cylinder decreases by increasing the thickness. Therefore, by

comparing curves of the Figs. 2 and 4 it is observed that by increasing the thickness, the amplitude of the radial displacement at the inner surface of the FGM cylinder increases. From Fig. 4 it may be noticed that the amplitude of the radial displacement of the alumina-aluminium FGM cylinder (n_1=2.4406 and n_2=0.4893) is less than that of FGM cylinder with n_1=n_2=5. Fig. 5 represents the time history of the radial displacement at the middle point of thick hollow FGM cylinder for various values of the power law exponents, for b/a=2.

Fig. 6 compares the time histories of the radial stress for different points of the hollow FGM cylinder along the thickness in a certain power law exponent (n=n_1=n_2=5), for b/a=1.2. It is observed that the radial stress on the inner and outer surfaces are equal to the imposed dynamic pressures $p_1(t)$ and $p_2(t)$, respectively. Fig. 7 represents the distribution of the radial stress across the thickness of the FGM cylinder for various values of the power law exponents at time t=0.001 s, for b/a=1.2. It can be seen that the values of the power law exponents have direct effect on the amplitude of the radial stress at the points across the thickness between boundary surfaces. The greatest amplitude of the radial stress belong to the hollow cylinder made of alumina-aluminium FGM (n_1=9.2875 and n_2=1.86).

Fig. 8 illustrates the time history of the radial stress at the middle point of the thick hollow FGM cylinder for various values of the power law exponents, b/a=1.2. As mentioned before, the value of the power law exponents influences directly on the amplitude of the radial stress at the middle point of the hollow FGM cylinders. A comparison between the time histories of the radial stress at different points of the hollow FGM cylinder across the thickness in a certain power law exponent (n=n_1=n_2=5), for b/a=2, is shown in Fig. 9. As for the FGM cylinders with thickness b/a=1.2, the radial stress on the inner and outer surfaces are equal to the imposed dynamic pressures $p_1(t)$ and $p_2(t)$, respectively. The time histories of the radial stress of the middle point of the thick hollow FGM cylinder are shown in Fig. 10for various values of the power law exponents (b/a=2). The direct effect of the value of the power law exponents on the amplitude of the radial stress at the middle point of the hollow FGM cylinders is clearly observed. Figs. 11 and 12 show the time histories of the hoop stress at the middle point of the thick hollow FGM cylinder for various values of the power law exponents and b/a=1.2 and b/a=2, respectively.

Since only internal pressure is exerted in the present example, the resulted radial and hoop stresses are negative and positive for all radii, respectively. Since the outer boundaries of the cylinders are free to move outward, positive radial displacements are generated. This conclusion is in agreement with results of Lame's equation for the corresponding static loading.

In the present example, the FGM cylinder experiences a forced vibration under an internal pressure that varies exponentially to converge to a specified pressure (p_0). Therefore, the vibration response is considerably affected by the particular or steady state response. For this reason, the overall amplitude of the vibration (i.e. the magnitude of the radial displacement and the magnitude of the radial and hoop stresses) as the imposed internal pressure increases with time exponentially to converge to the steady state response (Figs.3, 5, 6, and 8 to 10). Since the system is considered to be conservative, the amplitude of the transient response does not decrease with time. Therefore, after a certain time, e.g. 5(ms), the transient oscillations are the dominant ones.

The transient response that is combined with the particular or quasi-static response is mainly composed of vibrations that are performed with the fundamental natural frequency of the FGM cylinder. In Figs. 6 and 8 t 10, effects of the higher vibration modes are also noticeable. So that, beat-type vibration is observed.

6. Conclusions

In the present paper, an exact elastodynamic solution is developed for the an infinitely long thick-walled FGM cylinder experiences plane-strain conditions, subjected to uniformly distributed dynamic pressures at the boundary surfaces. It is assumed that the material properties vary through the thickness according to a power law function. The presented analytical solution has the following advantages:

(1) In contrast to the previous works (e.g. references [28,29]), the thick-walled FGM cylinder is not divided into isotropic sub-cylinders. Therefore, the stress continuity condition is satisfied automatically through the proposed solution procedure. Hence, more accurate results will be obtained. Discontinuity of the radial stress component is almost exists in all finite element models proposed so far unless Hermitian elements are employed (Shariyat, 2008).

(2) For each of the quasi-static and the dynamic parts of the solution, analytical solutions are presented separately that make the problem to be solved easily. Therefore, the steady state response or the particular solution may be distinguished from the transient response.

(3) The proposed method is suitable for hollow plane-strain FGM cylinders with arbitrary thickness and arbitrary initial conditions, subjected to arbitrary forms of axisymmetric dynamic loads at the boundary surfaces.

(4) In the traditional finite element models, the cylinder is discretized to considerable degrees of freedom. Furthermore, time history of the variations of the displacement and stress components requires division of the time domain into many time steeps that are much less than the period time of the fundamental natural frequency of the cylinder [35] (usually of an order that varies between 10^{-6} and 10^{-5} (s) for the FGM cylinders, as results of tables 1 to 3 imply). Hence, the governing equations of the entire finite element model should be solved for a very large number of time steps. Therefore, in comparison to the traditional finite element methods, less computational time and memory allocation are required for the present solution procedure. Moreover, the traditional time integration methods induce numerical damping or numerical instability and may lead to considerable accumulated errors.

References

[1] Jabbari, M., Sohrabpour, S., and Eslami, M.R., "Mechanical and Thermal Stresses in a Functionally Graded Hollow Cylinder Due to Radially Symmetric Loads," International Journal of Pressure Vessle and Piping, Vol. 79, pp. 493–497, (2002).

[2] Jabbari, M., Sohrabpour, S., and Eslami, M.R., "General Solution for Mechanical and Thermal Stresses in a Functionally Graded Hollow Cylinder Due to Nonaxisymmetric Steady-state Loads," ASME Journal of Applied Mechanics, Vol. 70, pp. 111–118, (2003).

[3] Jabbari, M., Bahtui, A., and Eslami, M.R., "Axisymmetric Mechanical and Thermal Stresses in Thick Short Length FGM Cylinders," International Journal of Pressure Vessels and Piping, Vol. 86, pp. 296-306, (2009).

[4] Kim, K.S., and Noda, N., "Green's Function Approach to Unsteady Thermal Stresses in an Infinite Hollow Cylinder of Functionally Graded Material," Acta Mechanica, Vol. 156, pp. 145–61, (2002).

[5] Liew, K.M., Kitipornchai, S., Zhang, X.Z., and Lim, C.W., "Analysis of the Thermal Stress Behavior of Functionally Graded Hollow Circular Cylinders," International Journal of Solids and Structures, Vol. 40, pp. 2355–2380, (2003).

[6] Awaji, H., and Sivakumar, R., "Temperature and Stress Distribution in a Hollow Cylinder of Functionally Graded Material: The Case of Temperature-independent Material Properties," Journal of American Ceramic Society, Vol. 84, pp. 1059–1065, (2001).

[7] Wang, B.L., Mai, Y.W., and Zhang, X.H., "Thermal Shock Resistance of Functionally Graded Materials," Acta Materialia, Vol. 52, pp. 4961–4972, (2004).

[8] Wang, B.L., and Mai, Y.W., "Transient One-dimensional Heat Conduction Problems Solved by Finite Element," International Journal of Mechanical Sciences, Vol. 47, pp. 303–317, (2005).

[9] Hosseini, S.M., Akhlaghi, M., and Shakeri, M., "Transient Heat Conduction in Functionally Graded Thick Hollow Cylinders by Analytical Method," Heat and Mass Transfer, Vol. 43, pp. 669–675, (2007).

[10] Shao, Z.S., Wang, T.J., and Ang, K.K., "Transient Thermo-mechanical Analysis of Functionally Graded Hollow Circular Cylinders," Journal of Thermal Stresses, Vol. 30, No. 1, pp. 81-104, (2007).

[11] Shao, Z.S., and Ma, G.W., "Thermo-Mechanical Stresses in Functionally Graded Circular Hollow Cylinder with Linearly Increasing Boundary Temperature," Composite Structures, Vol. 83, pp. 259–265, (2008).

[12] Santos, H., Mota Soares, C.M., Mota Soares, C.A., and Reddy, J.N., "A Semi-Analytical Finite Element Model for the Analysis of Cylindrical Shells Made of Functionally Graded Materials Under Thermal Shock," Composite Structures, Vol. 86, pp. 10-21, (2008).

[13] Shariyat, M., "Dynamic Thermal Buckling of Suddenly Heated Temperature-Dependent FGM Cylindrical Shells, Under Combined Axial Compression and External Pressure," International Journal of Solids Structures, Vol. 45, pp. 2598–2612, (2008).

[14] Bagri, A., and Eslami, M.R., "A Unified Generalized Thermoelasticity; Solution for Cylinders and Spheres," International Journal of Mechanical Sciences, Vol. 49, pp. 1325–1335, (2007).

[15] Bagri, A., and Eslami, M.R., "Generalized Coupled Thermoelasticity of Functionally Graded Annular Disk Considering the Lord–Shulman Theory," Composite Structures, Vol. 83, pp. 168–179, (2008).

[16] Hosseini, S.M., Akhlaghi, M., and Shakeri, M., "Heat Conduction and Heat Wave Propagation in Functionally Graded Thick Hollow Cylinder Based on Coupled Thermoelasticity without Energy Dissipation," Heat and Mass Transfer, Vol. 43, pp. 669–675, (2007).

[17] Heyliger, P., and Jilania, A., "The Free Vibration of Inhomogeneous Elastic Cylinders and Spheres," International Journal of Solids and Structures, Vol. 29, pp. 2689–2708, (1992).

[18] Han, H., Liu, G.R., Xi, Z.C., and Lam, K.Y., "Transient Waves in a Functionally Graded Cylinder," International Journal of Solids and Structures, Vol. 38, pp. 3021-3037, (2001).

[19] El-Raheb, M., "Transient Waves in an Inhomogeneous Hollow Infinite Cylinder," International Journal of Solids and Structures, Vol. 42, pp. 5356–5376, (2005).

[20] Ponnusamy, P., "Wave Propagation in a Generalized Thermoelastic Solid Cylinder of Arbitrary Cross-Section," International Journal of Solids and Structures, Vol. 44, pp. 5336–5348, (2007).

[21] Shakeri, M., Akhlaghi, M., and Hoseini, S.M., "Vibration and Radial Wave Propagation Velocity in Functionally Graded Thick Hollow Cylinder," Composite Structures, Vol. 76, pp. 174–181, (2006).

[22] Hosseini, S.M., Akhlaghi, M., and Shakeri, M., "Dynamic Response and Radial Wave Propagation Velocity in Thick Hollow Cylinder Made of Functionally Graded Materials," Engineering Computations: International Journal for Computer-Aided Engineering and Software, Vol. 24, No. 3, pp. 288-303, (2007)

[23] Hosseini, S.M., "Coupled Thermoelasticity and Second Sound in Finite Length Functionally Graded Thick Hollow Cylinders (without Energy Dissipation)," Materials and Design, Vol. 30, pp. 2011-2023, (2008).

[24] Bruck, H.A., "A One-dimensional Model for Designing Functionally Graded Materials to Manage Stress Waves," International Journal of Solids and Structures, Vol. 37, pp. 6383-6395, (2000).

[25] Samadhiya, R., Mukherjee, A., and Schmauder, S., "Characterization of Discretely Graded Materials using Acoustic Wave Propagation," Computational Materials Science, Vol. 37, pp. 20-28, (2006).

[26] Shariyat, M., "A Nonlinear Hermitian Transfinite Element Method for Transient Behavior Analysis of Hollow Functionally Graded Cylinder with Temperature-Dependent Materials under Thermo-Mechanical Loads," International Journal Pressure Vessel and Piping, Vol. 86, pp. 280-289, (2009).

[27] Tutuncu, N., "Stresses in Thick-Walled FGM Cylinders with Exponentially-varying Properties," Journal of Engineering Structures, Vol. 29, pp. 2032-2035, (2007).

[28] Yue, Z.Q., and Yin, X.C., "Transient Plane-Strain Response of Multilayered Elastic Cylinders to Axisymmetric Impulse," ASME Journal of Applied Mechanics, Vol. 2002, No. 69, pp. 825-835, (2002).

[29] Ding, H.J., Wang, H.M., and Chen, W.Q., "Elastodynamic Solution for Spherically Symmetric Problems of a Multilayered Hollow Sphere," ASME Journal of Applied Mechanics, Vol. 73, pp. 753-768, (2004).

[30] Tang, L., and Cheng, J., **"**An Eigenfunction Expansion Method for the Elastodynamic Response of an Elastic Solid with Mixed Boundary Surfaces," Progress in Natural Science, Vol. 18, No. 9, pp. 1063-1068, (2008).

[31] Eringen, A.C., and Suhubi, E.S., "*Elastodynamics*", Vol. 2, *Linear Theory*, Academic press, New York, pp. 440, (1975).

[32] Rao, S.S., "Vibration of Continuous Systems," Wiley, New York, (2007).

[33] Fung, Y.C., and Tong, P., "*Classical and Computational Solid Mechanics*," World Scientific Pub Co Inc. (2002).

[34] Rade, L., and Westergren, B., "*Mathematics Handbook for Science and Engineering*," Springer-Verlag publishers, Berlin, fifth edition (2004).

[35] Bathe, K.J., "*Finite Element Procedures*," Prentice Hall, Englewood Cliffs, New Jersey, (2007).

Nomenclature

a	inner radius of the cylinder
A,B	time-dependent coefficient
b	outer radius of the cylinder
c_1, c_2	elastic coefficients
D	coefficient
E, E_0	Young's modulus, reference, Young's modulus
k	dimensionless natural frequency
J	Bessel's function of the first kind
m	number of the wave modes
n, n_1, n_2	exponents of the power law functions
p_1, p_2	internal, external pressures
p*	pressure amplitude
P, P_0	property, the reference property defined at the outer surface
q	power
r	radius
t,t_0	time, final time
u, u_0	radial displacement, initial value of the radial displacement
u_{st},u_{dy}	quasi-static, dynamic parts of the radial displacement expression
U_i	the *i*th wave mode
v,v_0	radial velocity, initial radial velocity
Y	Bessel's function of the 2nd kind

Greek symbols

α	an expression
β	element of the eigenvector
ε	an expression of Bessel functions
ε_r,ε_θ	radial, circumferential strains
Φ	a function
η	root of the characteristic equation
λ	coefficient
Λ_1,Λ_2	expressions of Bessel's functions
ν	Poison's ratio
ρ, ρ_0	the mass density, reference mass density
σ_r,σ_θ	radial, hoop stresses
ξ	ratio of the reference elastic coefficients
ω	frequency
Ψ	time-dependent coefficient

Figures

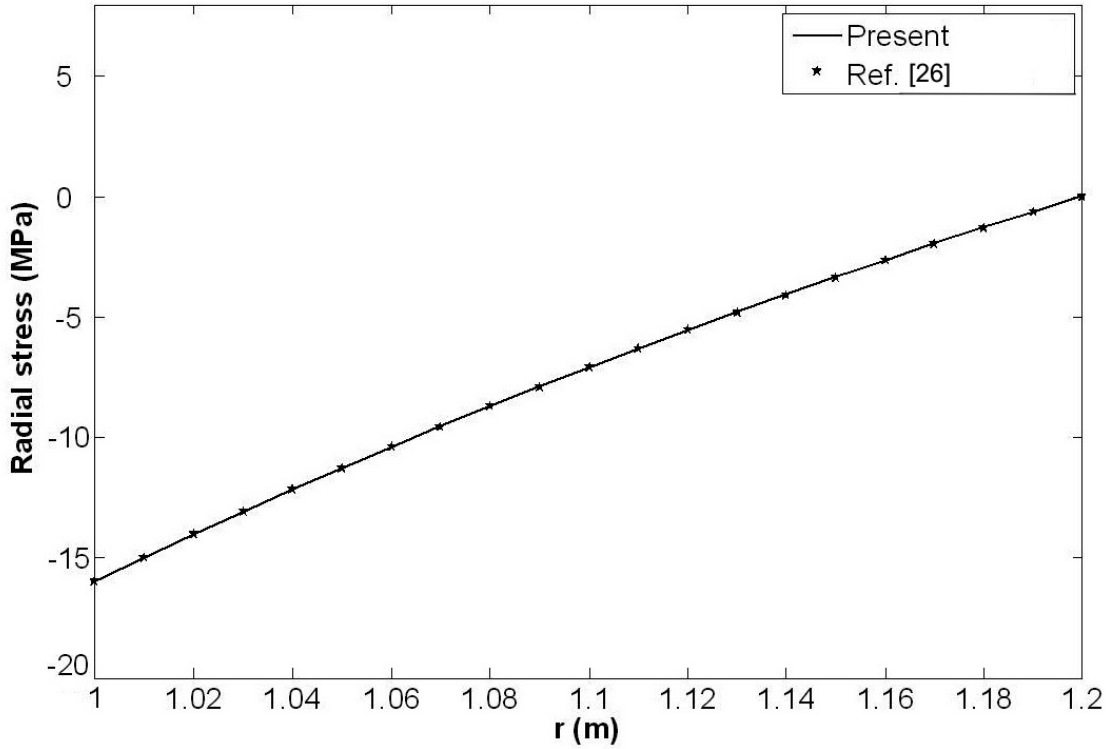

Figure. 1 Distribution of the radial stresses of a FGM thick cylinder subjected to an internal pressure that varies linearly with time, for (n_1=n_2=0.5, b/a=1.2, and t=0.004s).

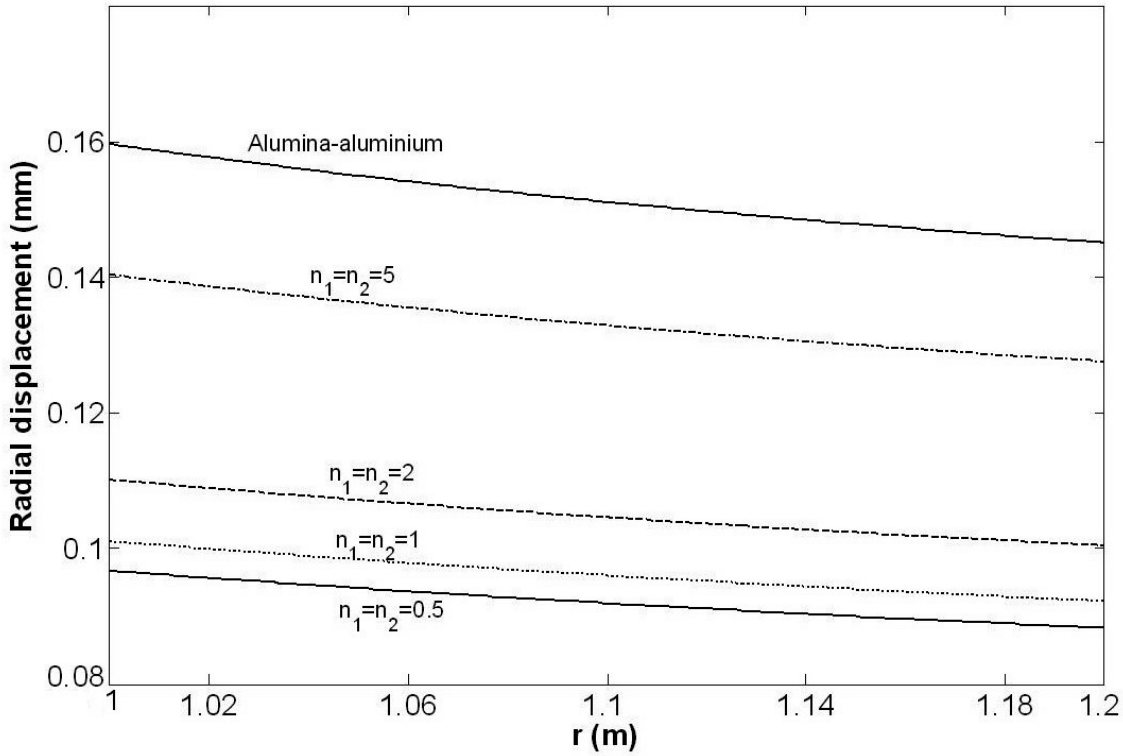

Figure. 2 Distribution of the radial displacement for different values of the power law exponent (b/a=1.2 and t=0.001s)

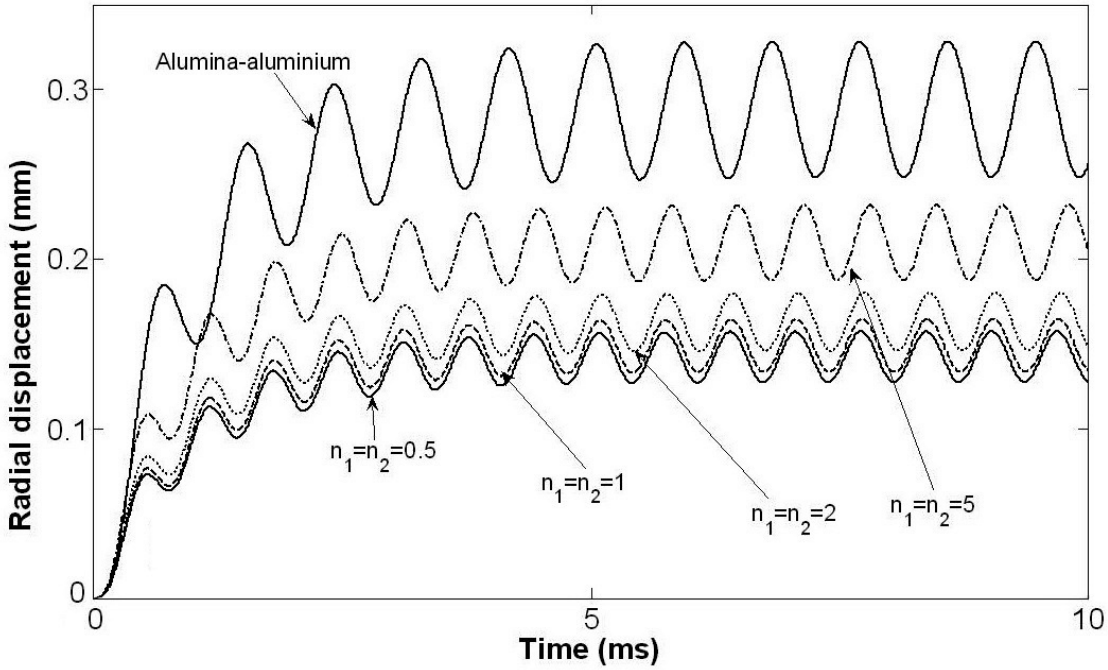

Figure. 3 Time history of the radial displacement of the middle point of the thickness of the FGM cylinder for various values of the power law exponent (*b/a=1.2*).

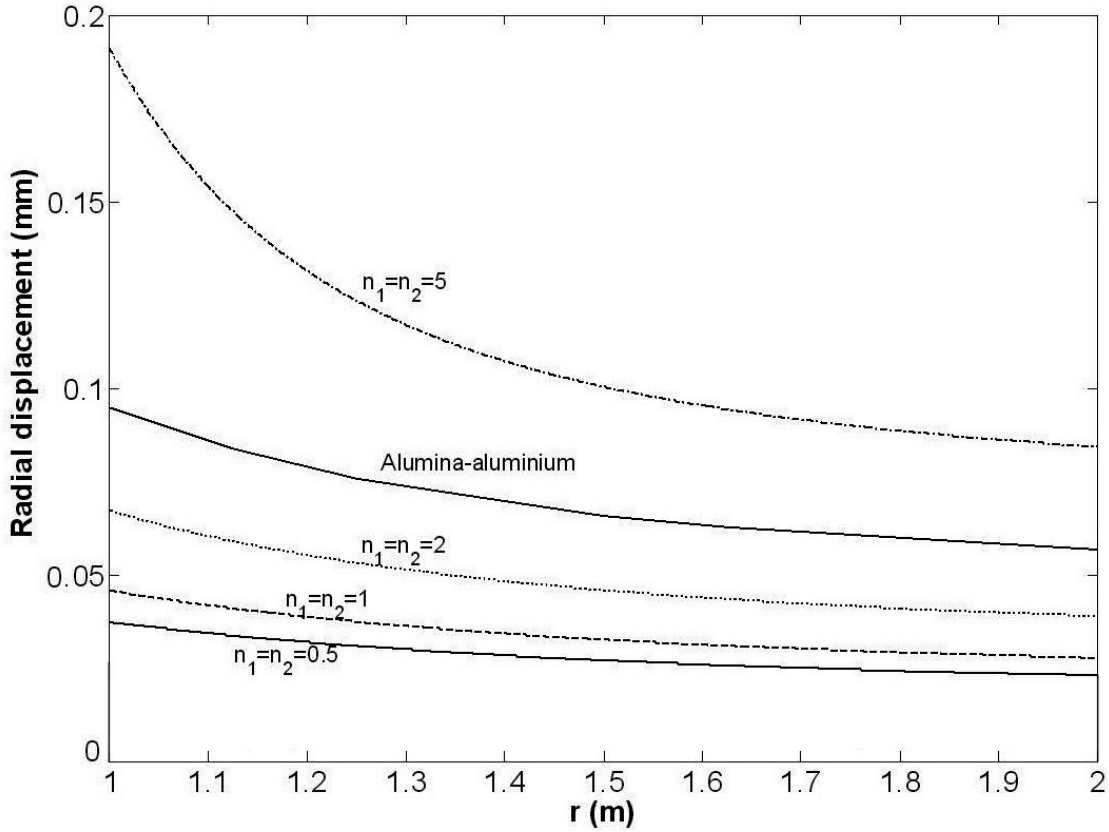

Figure. 4 Distribution of the radial displacement for different values of the power law exponent (*b/a*=2 and *t=0.001s*)

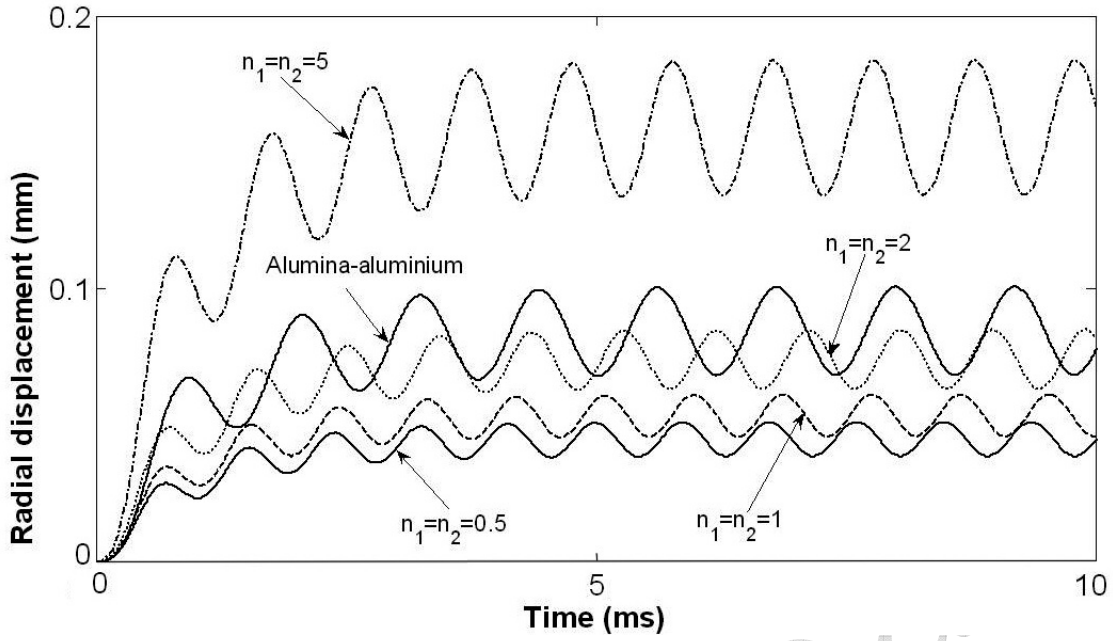

Figure. 5 Time history of the radial displacement of the middle point of the thickness of the FGM cylinder for various values of the power law exponent (*b/a=2*).

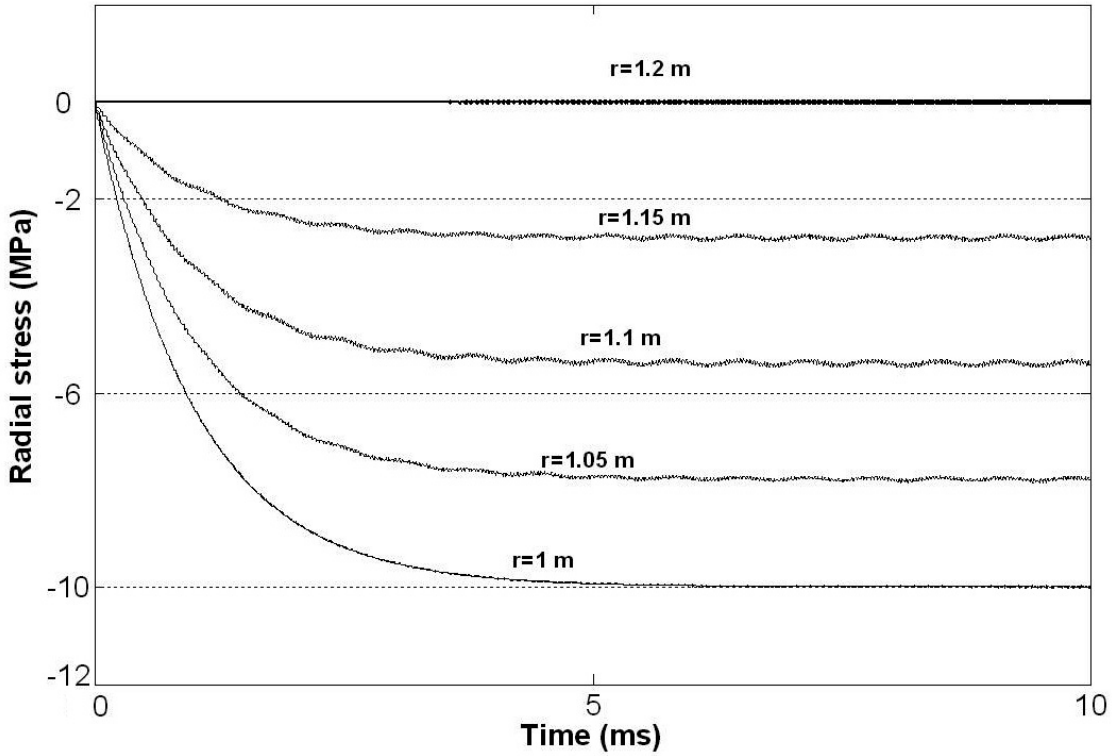

Figure. 6 Time histories of the radial stress for different points of the thickness of the FGM cylinder ($n_1=n_2=5$ and $b/a=1.2$)

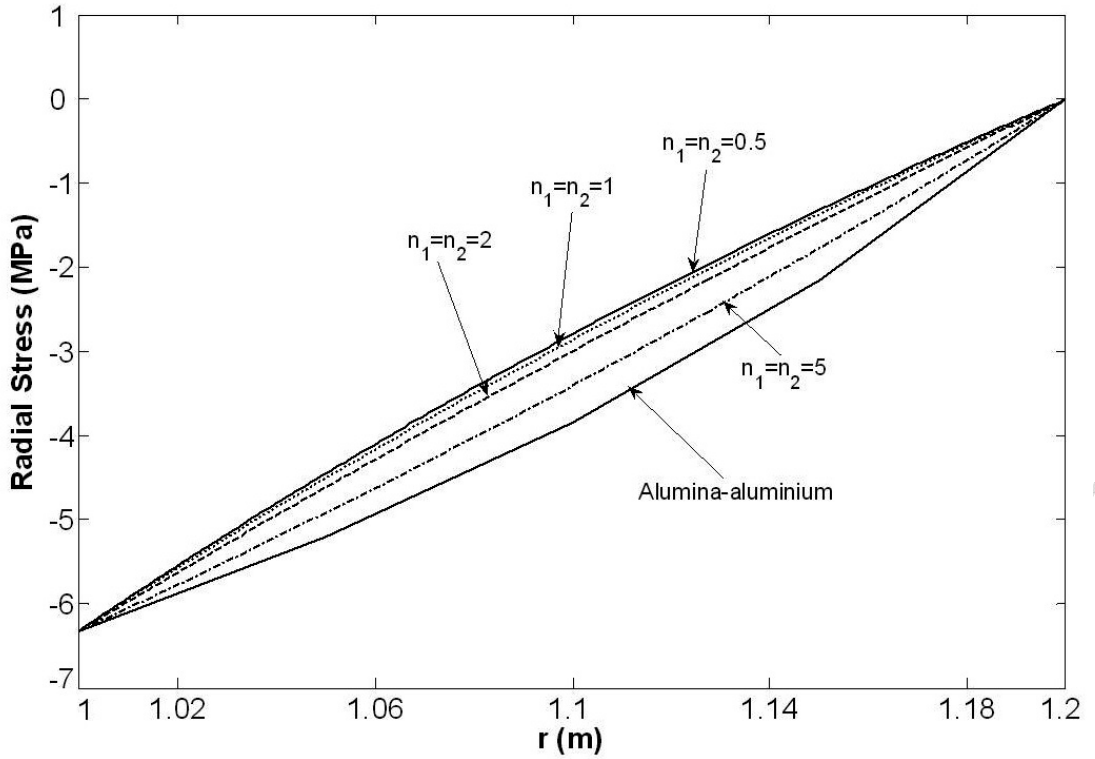

Figurre. 7 Distribution of the radial stress of the FGM cylinder for various values of the power law exponent at *t=0.01s* (*b/a=1.2*).

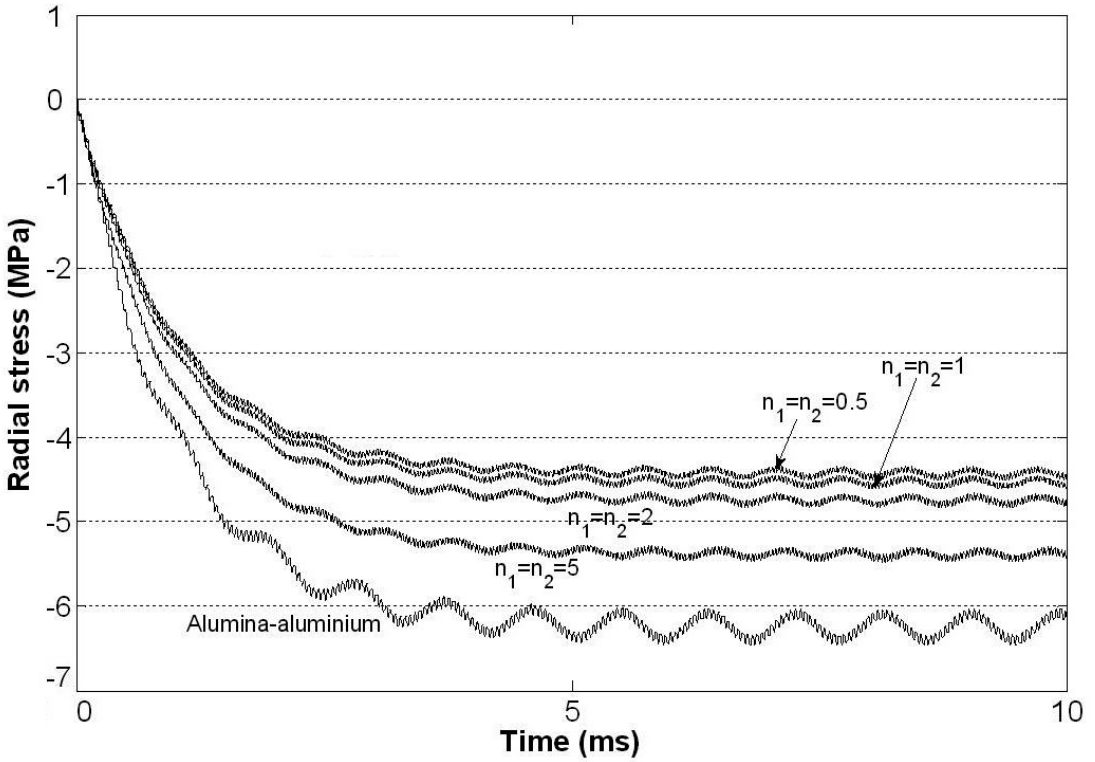

Figure. 8 Time history of the radial displacement of the middle point of the thickness of the FGM cylinder for various values of the power law exponent (*b/a=1.2*).

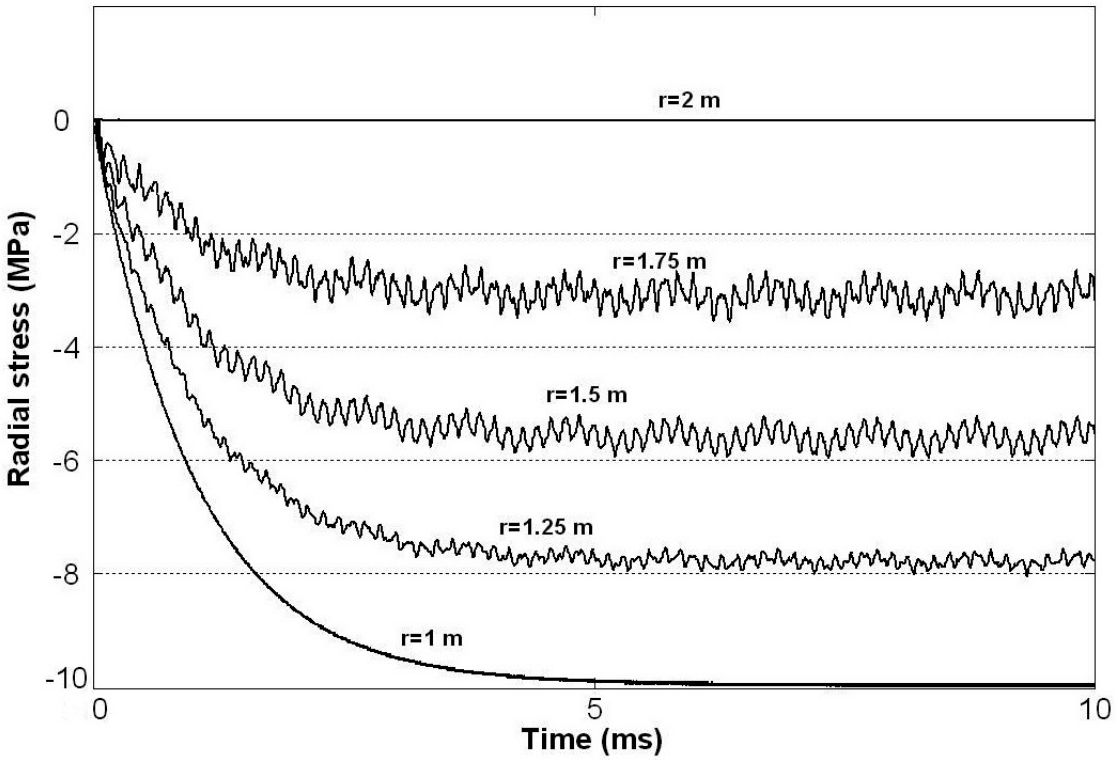

Figure. 9 Time histories of the radial stress of different points of the thickness of the FGM cylinder for $n_1=n_2=5$ ($b/a=2$).

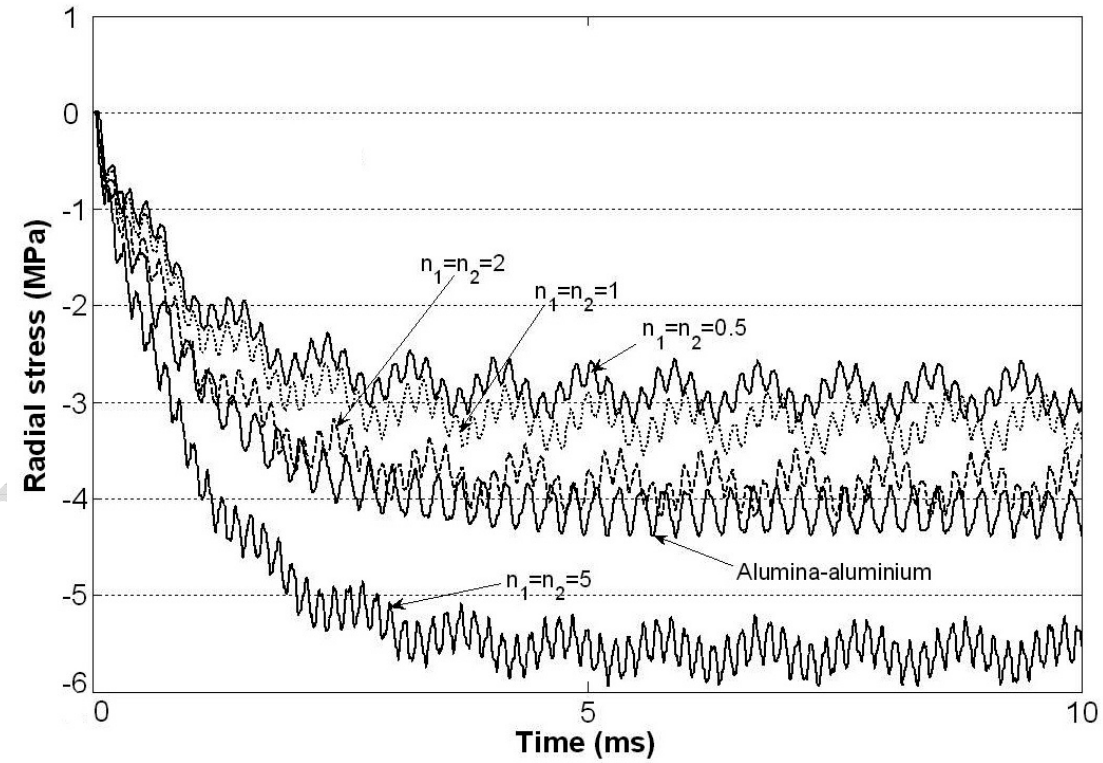

Figure. 10 Time histories of the radial stress of the middle point of the thickness of the FGM cylinder for various values of the power law exponent ($b/a=2$).

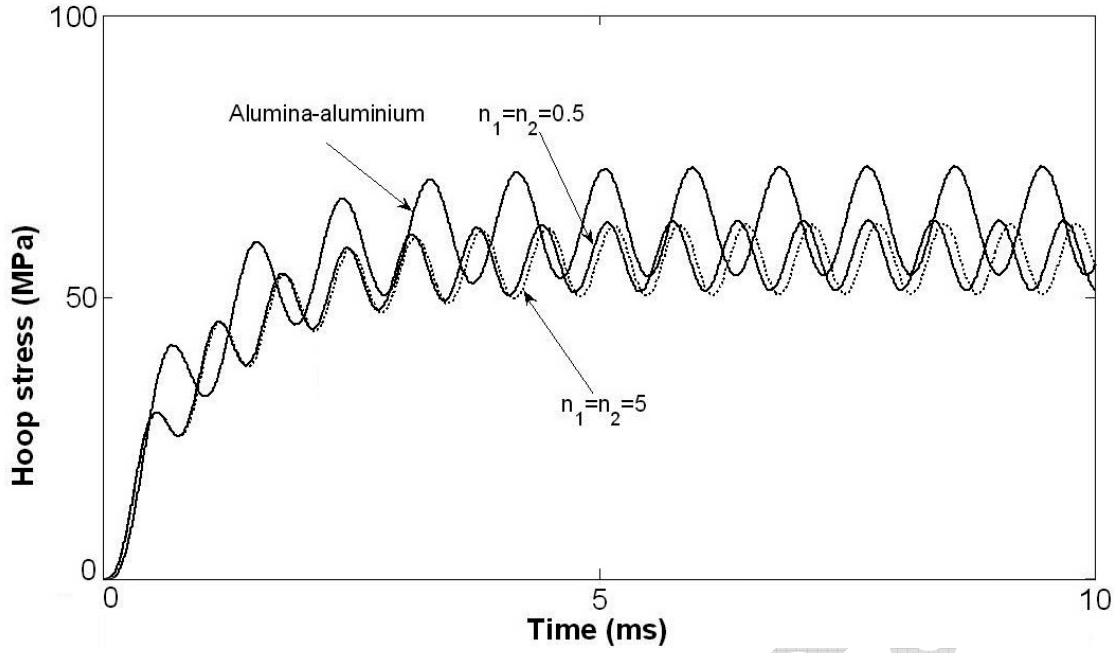

Figure. 11 Time histories of the hoop stress of the middle point of the thickness of the FGM cylinder for various values of the power law exponent (*b/a=1.2*).

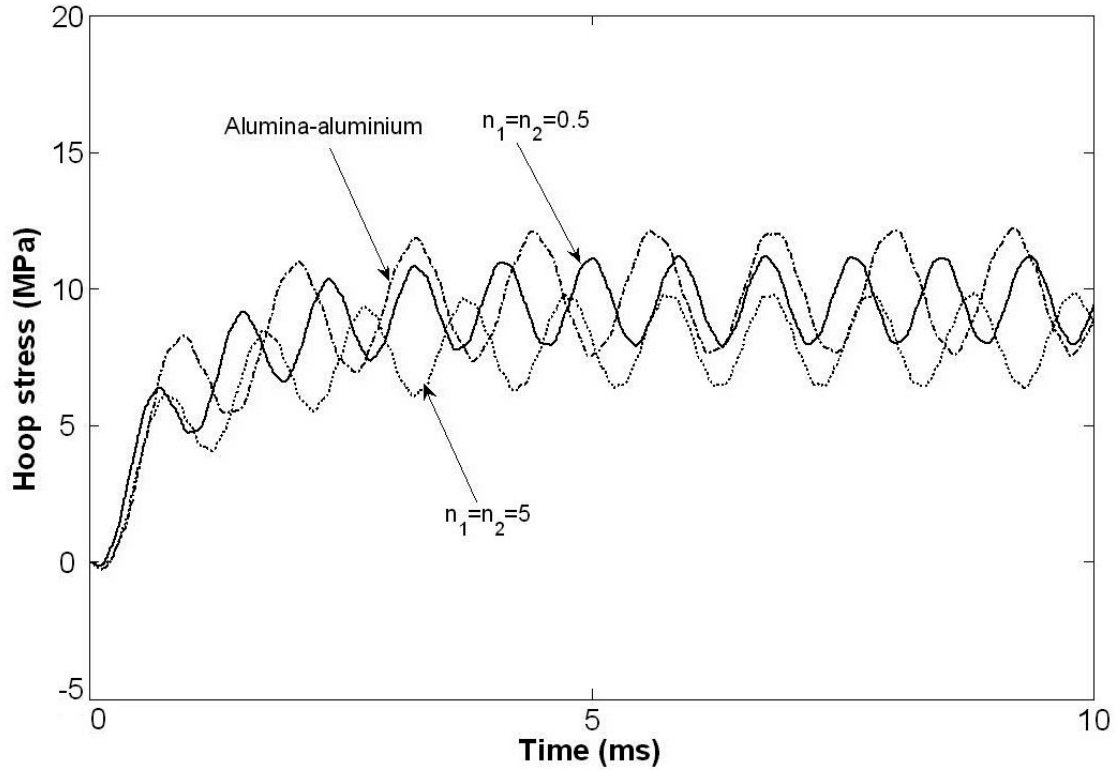

Figure 12 Time histories of the hoop stress of the middle point of the thickness of the FGM cylinder for various values of the power law exponent (*b/a=2*).

Tables

Table 1 The first six frequencies of FGM hollow cylinder for *b/a*=1.2.

Frequency(Hz)	*n*=0.5	*n*=1	*n*=2	*n*=5
ω_1	9552	9539	9513	9436
ω_2	182632	182777	183181	185293
ω_3	364691	364763	364966	366034
ω_4	546870	546925	547061	547774
ω_5	729095	729131	729233	729768
ω_6	911326	911355	911436	911864

Table 2 The first six frequencies of FGM hollow cylinder for *b/a*=1.5.

Frequency(Hz)	*n*=0.5	*n*=1	*n*=2	*n*=5
ω_1	8481	8424	8312	8013
ω_2	73671	73955	74740	78722
ω_3	146183	146328	146731	148835
ω_4	218955	219052	219322	220740
ω_5	291791	291864	292066	293133
ω_6	364653	364711	364873	365728

Table 3 The first six frequencies of FGM hollow cylinder for *b/a*=2.

Frequency(Hz)	*n*=0.5	*n*=1	*n*=2	*n*=5
ω_1	7204	7066	6810	6236
ω_2	37624	38028	39116	44303
ω_3	73478	73692	74286	77333
ω_4	109733	109878	110278	112374
ω_5	146087	146196	146499	148085
ω_6	182479	182566	182809	184085

چكيده

در مقاله كنوني، حل دقيقي براي پاسخ گذراي استوانه جدار ضخيم داراي طول نامحدود ساخته شده از مواد FGM، در معرض فشارهاي ديناميكي در سطوح مرزي، براي شرايط اوليه دلخواه ارائه شده است. فرض شده است كه استوانه، داراي شرايط كرنش صفحه‌اي بوده و فشارهاي ديناميكي به طور يكنواخت و متقارن بر مرزهاي استوانه وارد آيند. همچنين فرض شده است كه خواص مواد در امتداد ضخامت، بر پايه يک تابع تواني تغيير نمايند. بر خلاف بسياري از پژوهشهاي پيشين، استوانه FGM به استوانه‌هاي جزء ايزوتروپيک تجزيه نشده است. از فرايند حلي مبتني بر بسط توابع گذراي موج بر حسب توابع ويژه، بهره گرفته شده است. عبارت جابجايي شعاعي ديناميكي به بخشهاي شبه استاتيكي و ديناميكي تجزيه شده و براي يافتن هر يک از بخشهاي ياد شده، روشي تحليلي ارائه شده است. بر اين پايه، توزيعهاي جابجايي شعاعي و مولفه‌هاي تنش در استوانه‌هاي جدار ضخيم براي مقادير مختلفي از توان تابع اختلاط مواد، نسبتهاي متفاوتي از شعاعهاي خارجي و داخلي و بارهاي ديناميكي گوناگون، بدست آمده‌اند. در پايان، برتريهاي روش پيشنهادي مورد بررسي قرار گرفته‌اند.